

# Allogeneic Descemet's Membrane Transplantation Enhances Corneal Endothelial Monolayer Formation and Restores Functional Integrity Following Descemet's Stripping

Maninder Bhogal,<sup>1-3</sup> Chan N. Lwin,<sup>1</sup> Xin-Yi Seah,<sup>1</sup> Gary Peh,<sup>1,4</sup> and Jodhbir S. Mehta<sup>1-5</sup>

<sup>1</sup>Tissue Engineering and Stem Cell Group, Singapore Eye Research Institute, Singapore

<sup>2</sup>Singapore National Eye Centre, Singapore

<sup>3</sup>Institute of Ophthalmology, University College London, London, United Kingdom

<sup>4</sup>Ophthalmology Academic Clinical Program, Duke-NUS Graduate Medical School, Singapore

<sup>5</sup>Department of Clinical Sciences, Duke-NUS Graduate Medical School, Singapore

Correspondence: Maninder Bhogal, Singapore National Eye Centre, 20 College Road, Singapore 168751; manibhogal@aol.com.

Submitted: April 24, 2017

Accepted: July 14, 2017

Citation: Bhogal M, Lwin CN, Seah X-Y, Peh G, Mehta JS. Allogeneic Descemet's membrane transplantation enhances corneal endothelial monolayer formation and restores functional integrity following Descemet's stripping. *Invest Ophthalmol Vis Sci*. 2017;58:4249-4260. DOI:10.1167/iops.17-22106

**PURPOSE.** To characterize the differences in corneal endothelial wound healing in the presence or absence of Descemet's membrane (DM), in vivo.

**METHODS.** New-Zealand white rabbits were subjected to 7-mm endothelial wound either by scraping ( $n = 8$ ; DM intact), peeling ( $n = 6$ ; DM removed), or a combinatory scrape/peel wound ( $n = 6$ ). In a second experiment, rabbits underwent peel wound with immediate transplantation of pure decellularized human DM ( $n = 4$ ). In vivo endothelial migration was assessed via trypan blue staining. Recovery of corneal clarity and thickness was performed by using slit-lamp biomicroscopy and optical coherence tomography. Cell proliferation, phenotype, and morphology were assessed by using immunofluorescence and scanning electron microscopy.

**RESULTS.** In vivo wound closure was faster in the presence of DM;  $25.4\% \pm 1.4\%/d$  versus  $5.5\% \pm 0.6\%/d$  ( $P < 0.0001$ ). At day 8, complete wound closure was seen in all of the scrape samples but none of the peel group, with wound closure preceding clinical recovery by approximately 6 days in the scrape group. Endothelial cells in the scraped areas reformed functional monolayers capable of restoring corneal thickness and transparency whilst those in the peeled area underwent mesenchymal-like transformation resulting in scar formation. Transplanting decellularized DM in animals receiving a peel wound resulted in clarity and thickness comparable to the scrape group. Endothelial proliferation (Ki67 +ve cells) was higher in scraped versus peeled areas:  $54.7\% \pm 3.5\%$  vs.  $8.8\% \pm 0.7\%$ , ( $P < 0.01$ ).

**CONCLUSIONS.** The presence of DM promoted endothelial wound healing, proliferation, and maintenance of a normal phenotype. DM transplantation recovered the abnormal peel phenotype back to that observed after endothelial scraping.

**Keywords:** corneal transplantation, Descemet's membrane transplantation, corneal endothelium

The cornea is the main refractive component of the eye responsible for focusing of light.<sup>1</sup> The ability to perform its function is predicated on having a functional layer of endothelial cells that pump water out of the corneal stroma, maintaining corneal clarity and shape.<sup>2</sup> In normal circumstances, in vivo, human corneal endothelial cells are maintained in a state of cell cycle arrest by a variety of mechanisms including contact inhibition and the effect of circulating inhibitors within the aqueous.<sup>3,4</sup> As a consequence, if endothelial cells are lost through damage or disease, corneal endothelial failure occurs, with the cornea swelling and losing its transparency.<sup>5</sup> Currently, the only treatment for endothelial failure is transplantation. In the United States, 48% of corneal transplants are for endothelial disease, establishing endothelial failure as the primary indication leading to transplantation.<sup>6</sup>

Corneal transplantation is not without complications,<sup>7</sup> and grafts have a finite lifespan,<sup>8,9</sup> meaning patients often have to

undergo more than one procedure.<sup>6</sup> Additionally, there is a global shortage of corneal transplant tissue, with approximately a third of the tissue collected being unsuitable for transplantation owing to poor endothelial quality.<sup>10</sup> Consequently, in recent years, focus has shifted toward efforts to help endothelial cells regenerate,<sup>11-14</sup> increasing the longevity of transplants, or bypassing the need for transplantation altogether.

The two leading causes of endothelial failure are Fuchs' endothelial dystrophy (FED) and pseudophakic bullous keratopathy (PBK).<sup>6</sup> Unlike PBK, in which there is widespread damage of the endothelial cells, endothelial damage in patients with FED seems to vary depending on the region of the cornea examined.<sup>15-17</sup> The disease is characterized by the presence of multiple excrescences, termed "guttatae," and thickening of DM and deposition of new layers of material forming the posterior banded layer and posterior collagenous layer. Guttatae are



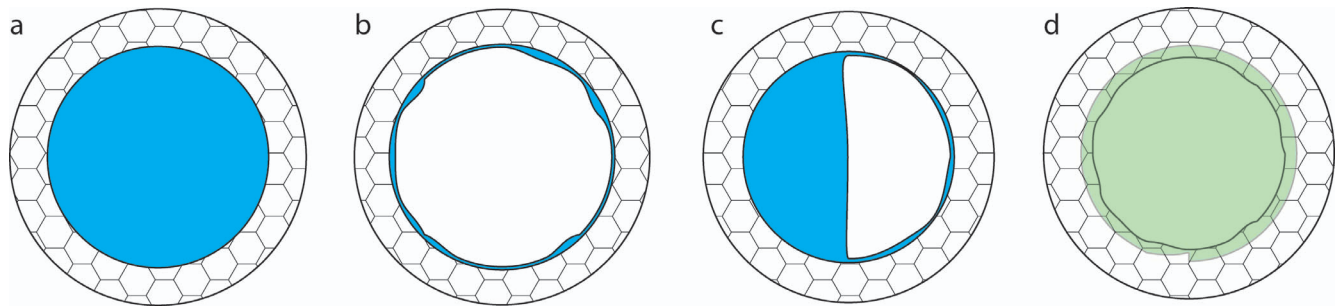


**FIGURE 1.** (a) Schematic showing scrape wound. The endothelial cells within a 7.00-mm mark are debrided, and confirmation of cell removal is witnessed by homogenous staining with trypan blue. (b) A peel wound is created by performing a 7.00-mm descemetorhexis. (c) Schematic of a half peel/half scrape wound. (d) DMT: after initial 7.00-mm descemetorhexis, an 8.0-mm decellularized Descemet's membrane is placed so that it fully overlaps the underlying peeled area.

primarily concentrated in the central cornea,<sup>16</sup> and as their density increases, corneal endothelial cell density typically reduces.<sup>18,19</sup> Even in patients with marked guttae and central corneal edema, the peripheral corneal endothelial cells can remain apparently healthy.<sup>20,21</sup> This potential reserve of healthy endothelial cells presents a possible pool of cells with the capacity to repopulate the central cornea.

Okumura et al.<sup>22</sup> have shown that it is possible to restore corneal clarity in patients with FED by first removing damaged endothelial cells by using cryotherapy, breaking contact inhibition, and then applying the Rho kinase inhibitor (ROCKI) Y-27632 topically. Whilst they show this strategy is successful in some patients with FED, it fails to work in those with iridoplasty-related bullous keratopathy, a variation of PBK, suggesting the effect likely involves migration of healthy cells from the reserve in the periphery.<sup>23-25</sup> However, a problem with this approach is that it leaves behind the guttae, which in addition to scattering light and degrading vision,<sup>26</sup> can have a significant negative impact on migration of endothelial cells.<sup>27</sup>

Hence, an alternative approach has been to perform a procedure termed “primary descemetorhexis.”<sup>24</sup> This involves the localized stripping of an area of Descemet's membrane (DM) to remove the central guttata, to allow the paracentral endothelial cells to migrate and hence reconstitute a central monolayer, and restore endothelial function.<sup>24,25</sup> Whilst it has been reported as successful in certain circumstances,<sup>24</sup> the time course of recovery can vary and success appears to be related to the age of the patient and the size of the descemetorhexis performed. To understand this process in more detail, we have previously investigated the effects of endothelial migration in an ex vivo model of endothelial damage in human corneas.<sup>28</sup> Our results show that human endothelial cell migration is significantly enhanced if the DM remains intact, irrespective of donor age. In the presence of an intact DM, supplementation of ROCKI has little effect in younger donors, but seems to encourage cell migration, which is otherwise slow, in older donors.

Endothelial cells are known to behave significantly differently in vivo than in in vitro/ex vivo environments, where culture media are supplemented with serum and growth factors.<sup>29</sup> In order to determine if the positive effects of maintaining DM observed ex vivo were preserved in vivo, we developed a wound healing model in the rabbit. We hypothesized that transplanting decellularised DM over an area of peeling would improve endothelial healing by providing a substrate more conducive to cell migration; a procedure we termed Descemet's membrane transplantation (DMT).

## METHODS

### Research Animals

Approval for the study was obtained from the Singhealth Institutional Animal Care and Use Committee. Animals were treated in accordance with the ARVO Statement for the Use of Animals in Ophthalmic and Vision Research. Interventions were performed in New Zealand white rabbits aged 16 to 20 weeks and weighing 3 to 3.5 kg. All surgical procedures and clinical evaluations were performed in single eyes of each rabbit under general anesthesia with intramuscular xylazine 5 mg/kg (Troy Laboratories, Smithfield, Australia) and ketamine 40 mg/kg (Parnell Laboratories, Alexandria, Australia) with additional topical anesthesia (lidocaine 1%; Bausch and Lomb, Bridgewater, NJ, USA). Before surgery, all rabbits were injected with intravenous unfractionated heparin (1000 IU in 1 mL normal saline) to prevent anterior chamber fibrin clot formation. At the designated time point, animals were euthanized with overdose intracardiac pentobarbitone and tissue was collected for postmortem analysis.

### Wound Creation

Three different wound types were used to evaluate the healing responses of endothelial cells in vivo: scrape, peel, and half scrape/half peel (Fig. 1) (Supplementary Video S1).

**Scrape.** The area of endothelial cells to be removed was marked with a 7.0-mm trephine to lightly score the epithelial surface. An anterior chamber infusion was used to prevent chamber collapse during the subsequent procedures. Endothelial cells were debrided by using a “mushroom” cataract instrument (Model No. 6-472; Duckworth and Kent, Baldock, UK) that had been altered to allow the smooth, ball-like, metallic surface to face the endothelium. Gentle rubbing of the endothelium for the entire area within the trephination mark was performed, followed by instillation of vision blue (DORC Ophthalmic, New Haven, CT, USA). Areas of debrided cells stained blue and were clearly visible intraoperatively. Any missed areas were debrided and staining repeated until complete endothelial cell removal had been achieved (Fig. 1a).

**Peel.** In the peel group, endothelial cells were initially debrided as above, as staining with trypan blue improved visualization for the subsequent steps. An initial flap in DM was created with the bent tip of a 27-gauge needle and continued with a blunt Sinsky hook or micro-coaxial forceps, taking care to follow the 7.0-mm epithelial mark. Care was taken not to disturb the underlying stroma and to remove all DM within the 7.0-mm zone (Fig. 1b).

**Half Scrape/Half Peel.** In this group, complete endothelial scraping was followed by DM removal from one semicircular half of the debrided area. This allowed comparisons of wound healing over areas covered with and free of DM within the same eye, mitigating any differences observed between individual rabbits (Fig. 1c) (Supplementary Video S1).

### Descemet's Membrane Transfer

Experimentation was conducted in accordance with the tenets of the Declaration of Helsinki. Human corneoscleral buttons with consent for research use were obtained from Miracles in Sight (Winston-Salem, NC, USA). Corneas were frozen overnight, whilst still within the viewing chamber, and subsequently thawed. This process was repeated twice before irrigating the endothelial surface copiously with balanced salt solution (BSS). Complete removal of endothelial cells from DM was confirmed with trypan blue and Hoechst staining in preliminary experimentation, with uniform staining of the DM with trypan blue (Vision Blue; DORC) indicating complete debridement of all endothelial cells.

DM grafts devoid of endothelial cells were prepared by using our previously described Descemet's membrane endothelial keratoplasty (DMEK) preparation and marking techniques.<sup>30,31</sup> In brief, the corneas were placed in a standard punch block (Coronet, Network Medical, UK) and 360° peripheral scoring was performed with a Sinsky hook. The DM was peeled 90% off, laid back flat, and punched with a 8.0-mm trephine. A triangular orientation mark was made in the periphery of the graft<sup>31</sup> before complete separation of the graft from the stroma and staining with 0.06% trypan blue surgical dye (Vision Blue) for 2 minutes. Excess dye was removed with cellulose sponges and tissue transferred to petri dish filled with BSS. Animals had a 7-mm descemetorhexis performed in the same manner as described for animals in the DM peel group above. Immediately following wound creation, the graft was drawn into a glass DMEK injector (Geuder, Heidelberg, Germany) and injected into the anterior chamber through a 2.8-mm, 2-step, limbal incision.

The graft was unfolded by using a standardized "no touch" technique and correct orientation confirmed with the triangular mark. DM grafts were centered, ensuring complete overlap with the area of peeled rabbit DM before injection of 20% sulphur hexafluoride. The corneal incision was closed with 10-0 nylon sutures (Fig. 1d).

### Postoperative Follow-up and Animal Euthanasia Schedule

Postoperative reviews were conducted on days 1, 3, 5, 7, 11, 14, 21, and 28. Examinations included slit-lamp biomicroscopy, anterior segment optical coherence tomography (OCT), and in vivo confocal microscopy at different time points. A grading scheme adapted from Proulx et al.<sup>32</sup> was used to assess graft transparency, with 4 indicating a clear graft; 3, a slight opacity with iris/lens details easily visible; 2, mild opacity with iris/lens details still visible; 1, moderate opacity with no iris/lens details; and 0, an opaque cornea (iris not visible).

Animals were killed at differing prespecified time points to allow analysis of wound healing, cell proliferation, tight junction formation, and changes in cell morphology at the appropriate time. The euthanasia time points and analysis performed are outlined in Supplementary Table S1.

### In Vivo Wound Closure Assessment

In vivo, endothelial wound healing was assessed by using intracameral trypan blue, a nontoxic viability dye used commonly

in cell culture, eye bank corneal assessment, and intraocular surgery. Eyes were dilated with cyclopentolate 1% and phenylephrine 2.5% before creation of a paracentesis and injection of 0.06% trypan blue dye. After 2 minutes, trypan blue was washed out with BSS and intraoperative, retroillumination photography performed. In some cases, filling the anterior chamber with air was useful in improving image acquisition. Images were exported to ImageJ (<http://imagej.nih.gov/ij/>; provided in the public domain by the National Institutes of Health, Bethesda, MD, USA) and the areas of trypan blue staining were manually selected and measured. This method was validated by comparing intracameral trypan blue assessment with immunofluorescence and scanning electron microscopy in rabbits immediately killed after in vivo assessment at the day 3 time point ( $n = 4$ ). Healing rate (% area/d) was calculated by dividing the percentage wound healing by the number of days since wounding and performed at day 3 and day 5.

### Immunofluorescence

Rabbit corneas were excised and fixed in 1% paraformaldehyde at room temperature for 5 minutes. Samples were washed in phosphate-buffered saline (PBS), incubated in 1% Triton X-100, and blocked in 10% goat serum for 1 hour. Samples were incubated with primary antibodies against ZO-1 (1:300; Invitrogen, Thermofisher, Waltham, MA, USA), alpha smooth muscle actin ( $\alpha$ -SMA) (1:100; Agilent, Santa Clara, CA, USA), or Ki67 (1:100; Thermofisher) for 12 hours at 4°C. The samples were washed in PBS three times and labeled with secondary anti-mouse Alexa Fluor 488 (1:500; Thermofisher), Hoechst (1:1000; Thermofisher), and Alexa Fluor 546-conjugated phalloidin (1:100) at room temperature for 2 hours, washed again and refixed in 3% paraformaldehyde. Radial incisions were created as necessary to allow flat mounting of the tissue in Prolog gold mounting medium. The entire graft was imaged by using  $\times 10$  objective lens of the Nikon TiE inverted fluorescence microscope (Tokyo, Japan).

### Scanning Electron Microscopy

Samples were fixed in glutaraldehyde 2% immediately after euthanasia. Corneas were washed twice in PBS for 10 minutes each before being immersed in 1% aqueous solution of osmium tetroxide (FMB, Singapore) for 2 hours at room temperature. Samples were then dehydrated by using increasing concentrations of ethanol (25%, 50%, 75%, 95% to 100% ethanol, with 95% and 100% concentrations being performed twice), underwent critical point drying with Bal-Tec dryer (Balzers, Liechtenstein), and were mounted on stubs secured by carbon adhesive tape before sputter coating with a 10-nm-thick layer of gold (Bal-Tec). All samples were examined with the JSM-5600 scanning electron microscope (JEOL, Tokyo, Japan).

### Postoperative Cell Density and Morphometry

Flat mount images were exported to ImageJ for analysis. Cell density measurements were derived by using at least 500 cells from Hoechst staining in confocal images. Hexagonality ratio (a measure of pleomorphism), coefficient of variation of cell area (a marker of polymegathism), and cell circularity (a marker of a normal endothelial morphology) were determined after cell borders had been delineated with ZO-1 or actin staining as a guide.

### Statistical Analysis

Continuous data were reported as mean  $\pm$  standard deviation and compared by using 2-way, Student's *t*-tests. Where

appropriate, paired sample analysis was performed. Ordinal and nonparametric data were reported as a median and interquartile range and compared by using the Mann-Whitney *U* test. When comparison between more than two groups was required, ANOVA (parametric) or Kruskal-Wallis (nonparametric) tests were used. Statistical significance was set at  $P < 0.05$  for all experimentation.

## RESULTS

### Endothelial Scraping Versus Peeling

Before surgery, no epithelial defects, inflammation, or neovascularization was noticed in any eyes.

### Central Corneal Thickness Recovery

Peeling induced significantly more corneal swelling than scraping, with day 1 central corneal thickness (CCT) being significantly higher in the peel group. CCT recovered rapidly in the corneal scrape group, with all eyes returning to a normal thickness by day 11. Corneal thickness was significantly higher in the peel group at all time points and, in contrast to corneas in the scrape group, failed to recover to a normal thickness even after 28 days (Fig. 2).

### Corneal Transparency and Tomography

Corneal transparency recovered rapidly in the scrape group and achieved that of the control eye by day 11 (Fig. 2). In contrast, corneal clarity failed to recover in the peel group, with corneas in this group being significantly more opaque at day 28 ( $P = 0.029$ ) (Fig. 2). Initial edema was more prominent in the peel group and epithelial bullae were observed.

In the peel group, the entire cornea was initially opaque, including the periphery that had not been damaged (Fig. 2c). By day 14 the periphery had cleared sufficiently to make the iris details visible but the central peeled area remained opaque. A scar could be seen forming on the posterior corneal surface on slit-lamp examination at this time point. The corneal scars were more clearly seen on infrared imaging and were smaller than the initial peeled area in all animals, with a diameter of approximately 5 mm (Fig. 2d, upper panel). OCT images of the deturgessed corneas in the scrape group were indistinguishable from those of unoperated control eyes at day 28. In the peel group, OCT images of the scar and stroma were both more hyperreflective than those of the stroma in control animals and the scrape group. In the half scrape/half peel group, corneal clarity was restored over the scrape area, whilst a scar developed over the peeled area (Fig. 2d, lower panel).

### In Vivo Wound Healing

Areas of bare DM/stroma seen with in vivo trypan blue staining corresponded well with those observed ex vivo with alizarin red S/trypan blue staining or scanning electron microscopy (Figs. 3a–c). Wound closure was faster in scraped areas, even in animals that had had half scrape/half peel wounds (Figs. 3d, 3e). Complete closure of the 7.0-mm wound was seen in 75% of cases on day 5, and in all samples by day 8 (average time to closure 5 days [5–8], median [interquartile range; IQR]) in the scrape group. In contrast, 0% of wounds had closed by day 8; 80% by day 21; and 100% by day 28 (average time to closure 14 days [11–24.5], median [IQR]) in the peel group,  $P = 0.0025$  (Fig. 3f). The rate of wound closure was significantly higher in the scrape group with a healing rate of  $25.4\% \pm 1.4\%/d$  compared to  $5.5\% \pm$

$0.59\%/d$  in the peel group ( $P < 0.0001$ ) (Fig. 3g). The healing layer of cells in the peel group was initially flat, but after migrating approximately 1 mm, it formed a multilayered scar, something not seen in the scrape group.

### Scanning Electron Microscopy and Immunofluorescence

**Assessment at Day 3.** Cells in the scrape group migrated as confluent sheets, whereas those in the peel group had a scalloped pattern to the leading edge that could be seen with in vivo trypan blue staining (Fig. 3e) on confocal immunofluorescence microscopy (Fig. 4a) and scanning electron microscopy (Fig. 4b). The percentage of cells undergoing proliferation, as gauged by Ki67 staining, was significantly higher in the scraped than the peeled areas within the same eye:  $54.7\% \pm 3.5\%$  vs.  $8.8\% \pm 0.7\%$ ,  $P = 0.002$  ( $n = 3$ ) (Fig. 4a). A comparison of cell shape showed marked differences between cells in corresponding regions of samples from the half peel/half scrape group. Cells in the scrape portion of the wound maintained a more hexagonal “endothelial” morphology with a cell circularity of  $0.69 \pm 0.016$ , whereas those in the peel group were significantly more elongated and “fibroblastic”; cell circularity was  $0.37 \pm 0.019$  ( $P < 0.001$ ) (Fig. 4b).

**Changes to the Endothelial Mosaic With Time.** Scrape Wound. Immunofluorescence staining of samples from animals killed at day 5 confirmed that endothelial wound healing observed with in vivo trypan blue staining corresponded with large confluent cells covering the entire surface of DM (Fig. 5a). Endothelial cells showed patchy, broken staining for ZO-1, suggesting incomplete formation of tight junctions, and did not have the typical cortical pattern of actin staining seen in mature monolayers. Over the following 6 days the endothelial monolayer remodeled, with tight junction staining for ZO-1 and the actin cytoskeleton more closely resembling the controls (Fig. 5a). Cells became significantly smaller and more circular over the 28 days (Figs. 5b, 5c), with a change in cell size occurring between day 5 (the point of wound closure) and day 11 (the point of recovery of corneal thickness to preoperative levels). A similar pattern of cell maturation was seen when examining a strip of cells from the periphery to the center of the wound, with the cells in the periphery (the first to heal) being smaller and more circular than those centrally (the last to heal) (Figs. 5d–f).

Peel Wound. Cells in the periphery of the peel wound started with an endothelial morphology (Fig. 4b) similar to that observed in the scrape group. As time progressed and cells migrated further, they became progressively more elongated and spindle-like, displaying a fibroblastic morphology. By day 28 a peripheral rim (approximately 1 mm) of phenotypically normal endothelial cells with a central multilayered scar was seen on scanning electron microscopy (Fig. 6a) and immunofluorescence (Supplementary Fig. S1). In contrast to those in the scrape groups, cells in the central wound area stained positively for  $\alpha$ -SMA (Fig. 6b) and did not express ZO-1 (results not shown).

### Descemet’s Membrane Transplantation

As we were concerned about possibly dislodging the transplant, in vivo trypan blue assessment of wound healing was not performed in animals after DMT. The procedure was performed without complication in all rabbits. The DMT adhered to the posterior corneal surface without requiring rebubbling in all cases.

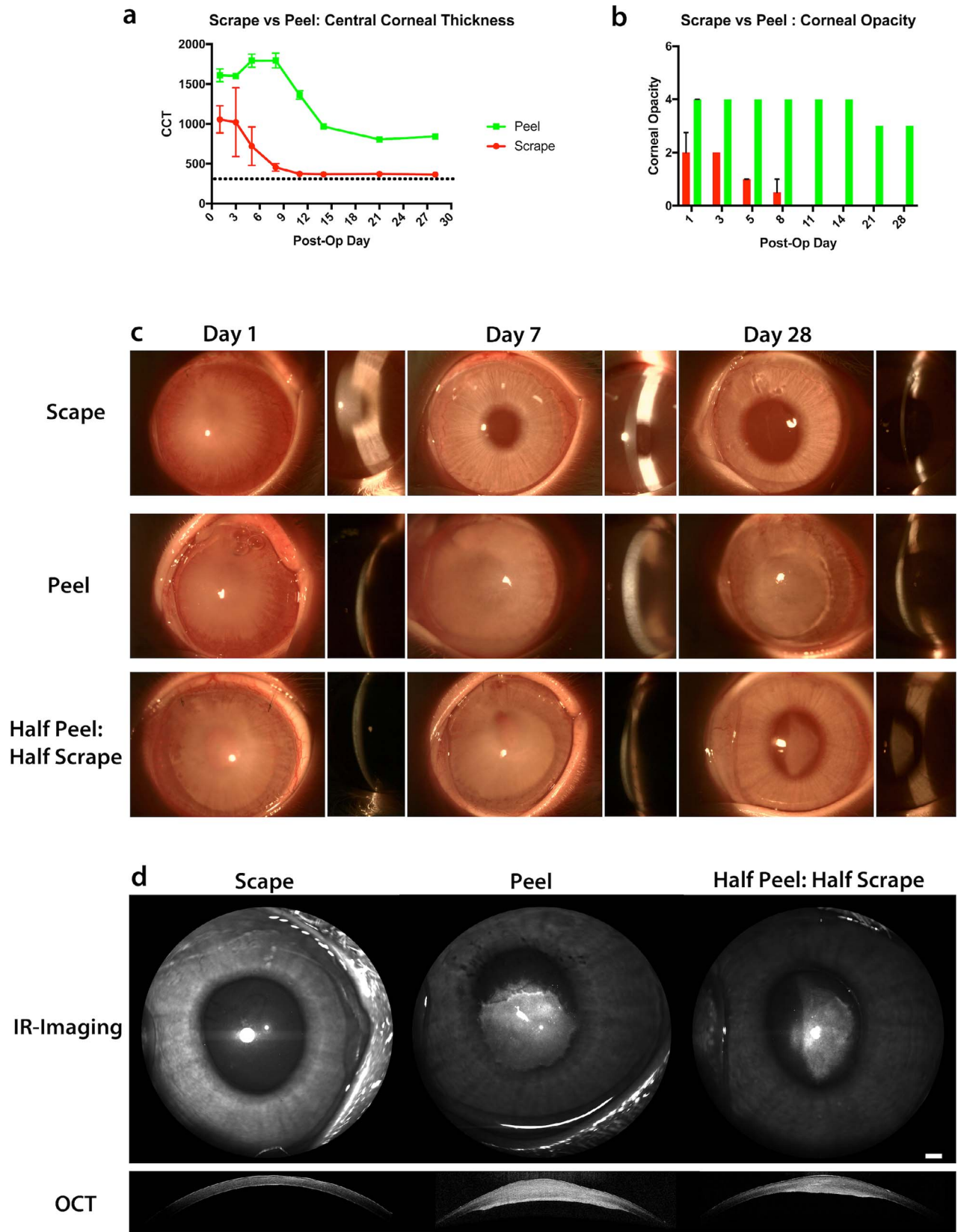


**FIGURE 2.** (a) Corneal thickness was significantly higher in peel group than in the scrape group at all time points. *Dotted line* represents the average prewounding central corneal thickness. (b) Corneal transparency rapidly returned to normal in the scrape group but failed to recover in the peel group. (c) Corneas in the scrape group healed without scarring, whereas those in the peel and half scrape/half peel group developed scars. (d) Corneal scars and overlying stroma were significantly more hyperreflective than the stroma of the scrape group on OCT imaging. *Scale bar*: 1 mm.

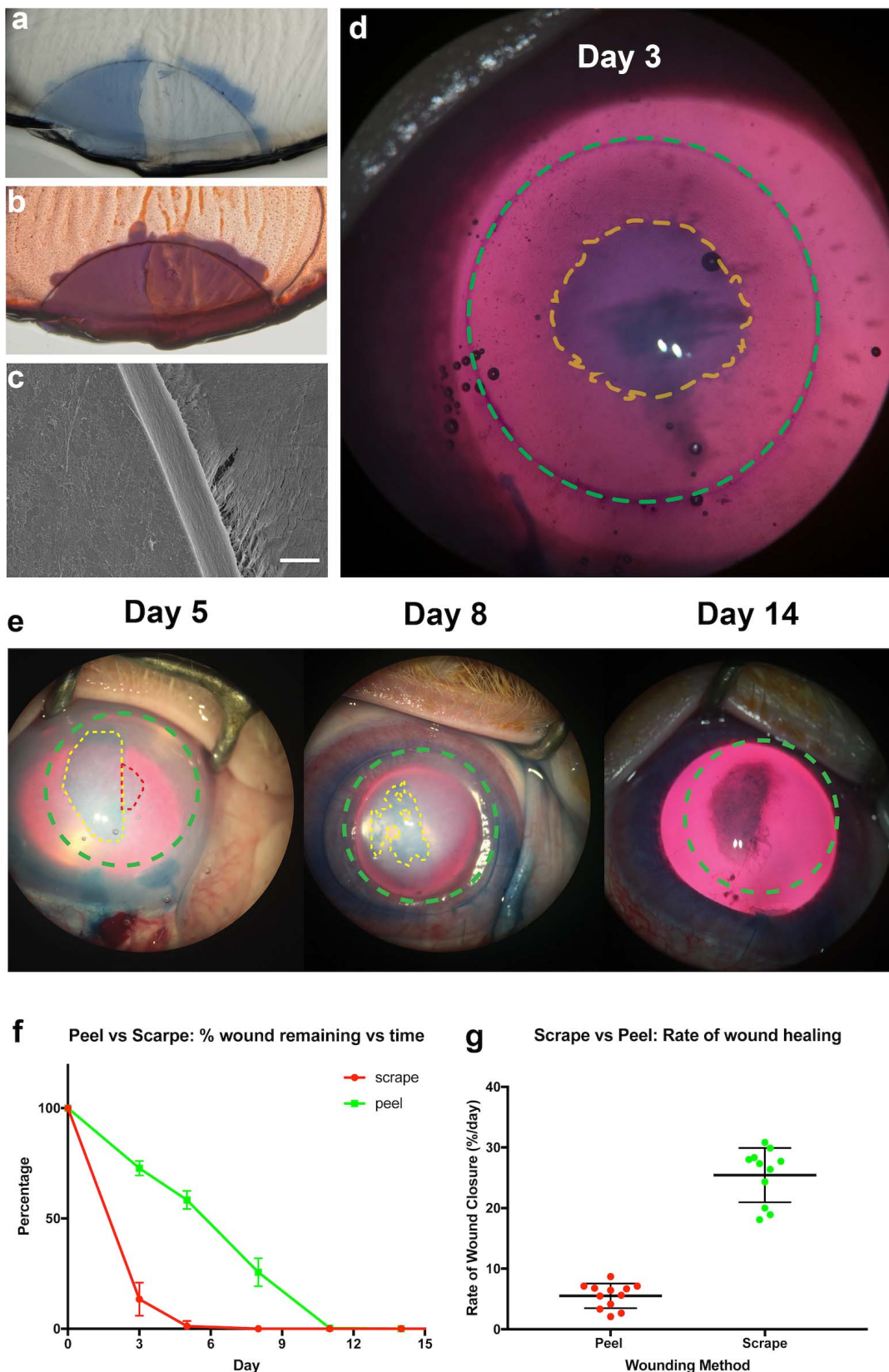


**FIGURE 3.** (a) Cornea recovered from a rabbit killed immediately after half scrape/half peel was performed, showing areas of denuded endothelium seen intraoperatively. (b) Restaining with trypan blue and alizarin red showed that the remaining peripheral endothelial cells were undamaged. (c) Scanning electron microscopy confirmed that both the peeled and scraped areas were devoid of endothelial cells. Scale bar: 10  $\mu$ m. (d) By day 3, considerable wound closure can be seen (yellow dashed line) in comparison to the original wound (green dashed line). (e) In serial imaging from the sample rabbit receiving a half scrape/half peel wound, endothelial wound healing was more complete in the scrape area (red dashed outline) than in the peeled area (yellow dashed outline). (f, g) Wound healing was significantly faster in the scrape group.

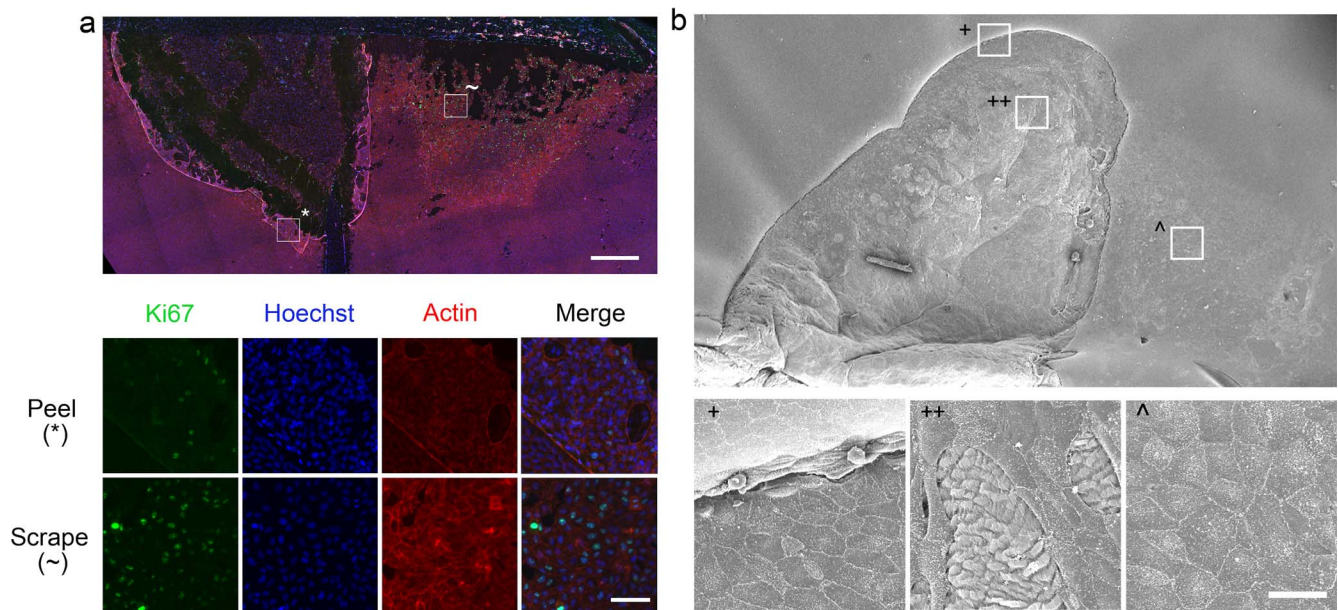


**FIGURE 4.** (a) *Upper panel:* Montage immunofluorescence image of a flat-mounted cornea from an animal killed at day 3 post half scrape/half peel wounding. Whilst endothelial cells in the scrape area have almost closed the wound, those in the peeled area have migrated much less. *Scale bar:* 1 mm. *Lower panel:* Higher magnification of areas outlined in the montage. A greater percentage of cells in the healing edge of the scrape wound are Ki67 +ve than those in the peeled area. *Scale bar:* 50  $\mu$ m. (b) Cell morphology differed between endothelial cells migrating over DM or bare stroma. Those migrating over DM retain a polygonal, endothelial morphology, whilst those migrating over the stroma become increasing elongated and fibroblastic the further they migrate. *Scale bar:* 25  $\mu$ m.

## Clinical Recovery

Corneal clarity was significantly better in the DMT group at day 28 than in the DM-peeled group ( $P = 0.04$ ), and was not different to that in animals undergoing endothelial scrape alone (DMT clarity of 0.25 (IQR: 0–1) (Figs. 7a, 7d). Unlike in the peel group, no central scarring was seen. However, a ring of opacification underneath the graft could be seen in the periphery of most samples on slit-lamp and OCT examination in the DMT group (Figs. 7b, 7c). In contrast to animals that had undergone peeling alone, in which all corneas remained swollen at day 28, CCT recovered to normal preoperative values after DMT had followed the recovery pattern observed in the scrape group (Fig. 7e). No significant differences in CCT were seen between the scrape and DMT groups at any time point (Fig. 7e).

## Electron Microscopy and Immunofluorescence

Endothelial cells migrated over the DMT graft, forming a confluent layer of polygonal cells (Fig. 7g) that displayed tight cell borders and microvilli on the cell surface (Fig. 7i), typical of a healthy endothelial mosaic. Examination of the area of opacification in the periphery of graft showed that endothelial cells trapped between transplanted and host layers of DM became fibroblastic with multiple actin stress fibers and positive expression for  $\alpha$ -SMA (Supplementary Video S2). Cell area was significantly higher in the DMT group than in scraped corneas at day 28 (Fig. 7e); however, hexagonality ratio and circularity were not statistically different for DMT and scrape samples.

## DISCUSSION

Our initial investigations comparing endothelial wound healing in the presence and absence of DM showed marked differences between these two groups. Using an in vivo imaging technique

adapted from our ex vivo experimentation, we observed that endothelial cells rapidly migrated over an intact healthy DM, with a 7.0-mm wound completely healing within 5 days. Following complete in vivo wound closure (day 5), the corneal thickness and clarity took another 6 days to recover (day 11). During that time the cells of the newly formed endothelial monolayer became significantly smaller with a greater expression of tight junction proteins as seen on immunohistochemistry. As this occurred, the endothelial barrier/pump function was restored with normalization of corneal thickness and clarity. In contrast, endothelial migration was significantly slower in cells moving over bare stroma. In the peel group, electron microscopy and immunofluorescence staining showed that cells typically preserved an “endothelial” morphology in the early stages of migration, approximately 1 mm from the peel edge. With further migration they became elongated, lost typical ZO-1 staining, and became positive for  $\alpha$ -SMA, features typical of endothelial-to-mesenchymal transformation. Eventually, these cells formed an opaque scar on the posterior stroma. Delayed wound closure with scarring has been reported by Arbelaez et al.<sup>53</sup> in three clinical cases of primary descemetorhexis. They note that this commonly occurred in areas in which the stromal bed had been inadvertently roughened during the peeling procedure. In our study central scarring was a consistent feature in the peel group. It was difficult to ascertain if this was due to smoothness of the underlying stroma (since care was taken to avoid stromal roughening by using forceps to remove tissue, meaning the DM could be gripped away from the posterior stroma), as opposed to a standard peeling technique. However, endothelial scarring was consistently seen in the peeling group and not the scraping group in our study.

In addition to enhancing endothelial cell migration, the presence of an intact basement membrane resulted in a significant increase in endothelial proliferation, measured by Ki67 staining. It is generally accepted that proliferation of human endothelial cells within a contact-inhibited monolayer

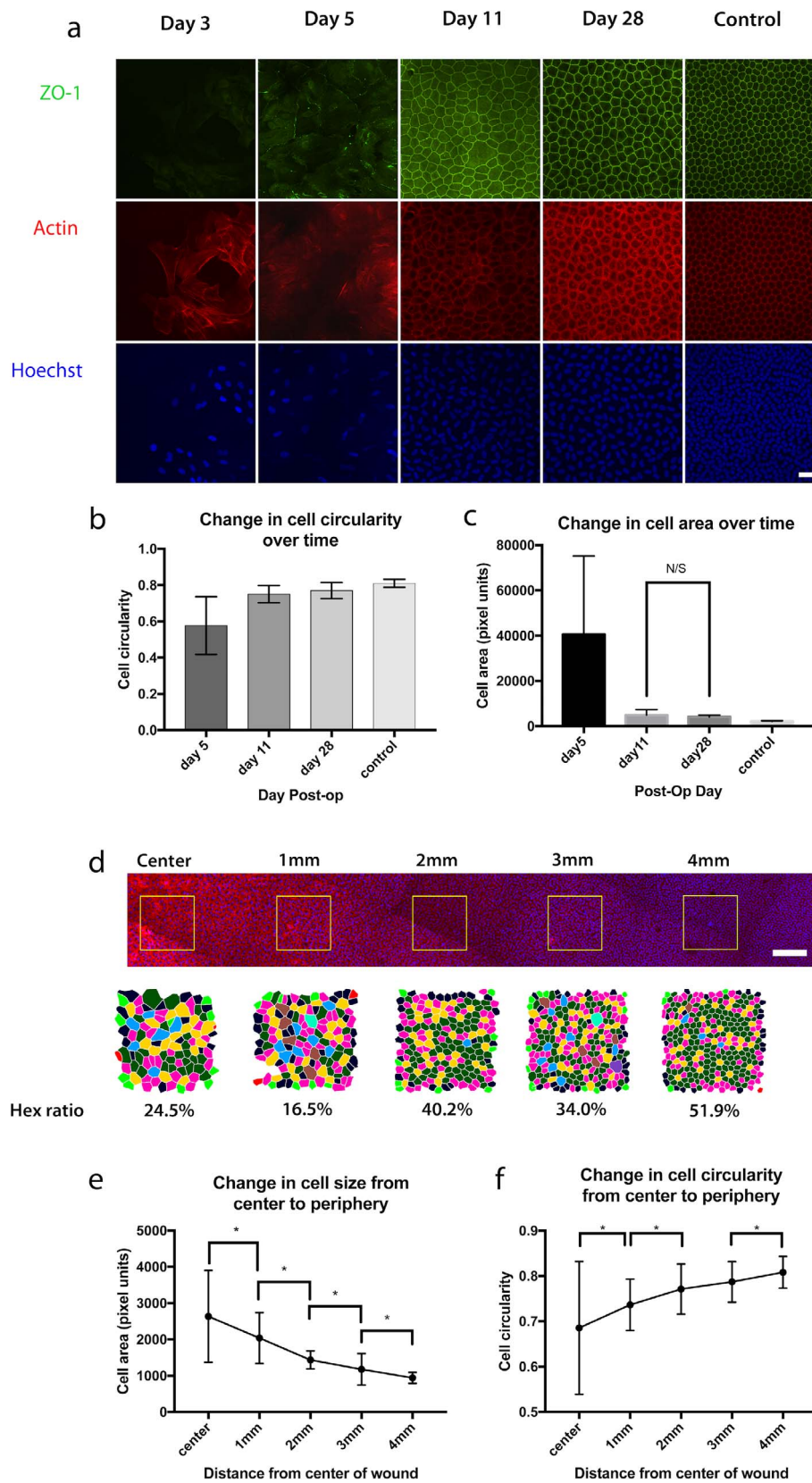


**FIGURE 5.** (a) Changes in the endothelial monolayer following scrape wounding occurred over time. At day 3, central cells are still spreading and closing the initial wound. By day 5, the cells have covered the wound completely but remain immature with limited ZO-1 expression at the junctions. At day 11, cells displayed polymegathism but stained strongly for ZO-1. By day 28, cells have become smaller and more regular. *Scale bar:* 50  $\mu$ m. As time progressed cells became more (b) circular (all comparisons between groups were significant with  $P < 0.01$ ) and (c) smaller (all comparisons between groups were significant with  $P < 0.01$  except between day 11 and day 28). (d) Differences in endothelial morphology are seen in different areas of the wound. The strip shows a montage of cells from the center (*left*) to the periphery of the 7-mm wound (*right*). The cells

from the areas outlined underwent neighbor analysis, with the results projected below. Those in the periphery, being the first to migrate, display a more “mature” architecture than those in the center, with smaller cells and a greater hexagonality ratio. *Scale bar*: 250  $\mu\text{m}$ . (e) Cells show progressive changes from the periphery to the center with those in the central cornea being significantly larger and (f) less circular (\* denotes an adjusted *P* value of  $<0.01$  for each comparison shown by the connecting bracket).

is insufficient to overcome ongoing cell loss *in vivo*. However, experiments examining endothelial wound healing in human eyes destined for enucleation have shown that endothelial proliferation does occur in human cells after wounding.<sup>34</sup> Although the level of proliferation in humans is likely to be significantly less than in rabbits,<sup>35</sup> treatment strategies using the regenerative ability of the peripheral reserve of human endothelial cells in conditions such as FED should seek to maximize any potential for proliferation *in vivo*.

We postulated that the differences observed between the peel and scrape groups could be influenced by increased inflammation and swelling in corneas that had had DM stripped. To account for this we examined wound healing and proliferation in corneas in which half the DM had been scraped and half peeled, therefore removing this confounding factor. The results mirrored those seen in animals in which the entire area had been either scraped or peeled, confirming that the presence of an intact DM was the main causative factor for the observed differences.

The rabbit endothelium is known to differ from that of humans, leading some to recommend the use of other animal models such as the cat<sup>35</sup> or cynomolgus monkey<sup>13</sup> for researching endothelial transplantation strategies and wound healing. However, the enhanced ability of rabbit endothelial cells to migrate allows examination of wound healing in a compressed time period, making the rabbit a useful model that has been used by several groups to explore the beneficial

effects of pharmaceutical treatment on corneal wound healing.<sup>15,36</sup> In the scratch group, the endothelial mosaic continued to mature over the first month, with a decrease in cell size and increase in hexagonality ratio. In addition to these temporal changes, spatial variations in cell density and hexagonality were seen within samples, with the cells at the center of the wound having a lower density than those at wound edge at day 28. These features show that remodeling of the endothelial monolayer continues to occur long after initial wound closure and restoration of pump function.

This phenomenon has been observed in human corneal endothelial cells after accidental descemetorhexis.<sup>23</sup> Consequently, it is plausible that the differences observed in the rabbit would be mirrored in human endothelial cells *in vivo*, albeit over a prolonged time scale. We have previously found that human endothelial cells migrate more slowly in peeled wounds than in scratched wounds *ex vivo*<sup>28</sup> in a similar fashion to what we have demonstrated here *in vivo*. In the same study, we have found that ROCK inhibition enhances wound healing, especially in elder donors, but only in the presence of an intact DM (over the time period we examined). Together these observations suggest that having an intact basement membrane is important if cell migration is to be optimized in regenerative strategies for corneal wound healing in conditions such as FED.

The DM in FED is characterized by the presence of guttae. In addition to degrading vision<sup>26</sup> and hindering endothelial

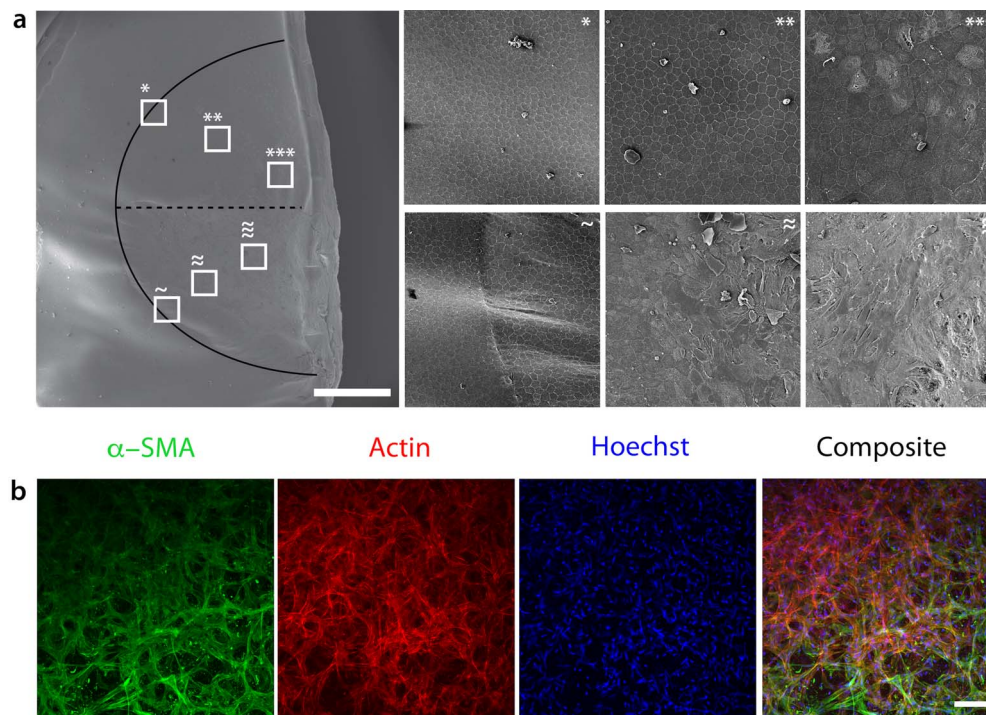


**FIGURE 6.** (a) Half scrape/half peel at day 28. The *black outline* denotes the area of wounding, the *dashed line* the distinction between the scraped and peeled areas. Cells in the entire scrape (\*, upper half of cornea) area retain an “endothelial” morphology, with polygonal monolayer cells visible on SEM. Endothelial cells in a peeled portion of the same cornea (*lower half*) start with an endothelial phenotype (~) but get more disorganized and fibroblastic as they migrate centrally (~~), eventually forming a multilayer scar (~~~). *Scale bar*: 1 mm. (b) Endothelial cells in the scar portion of the scrape have undergone EMT and express  $\alpha$ -SMA. *Scale bar*: 50  $\mu\text{m}$ .

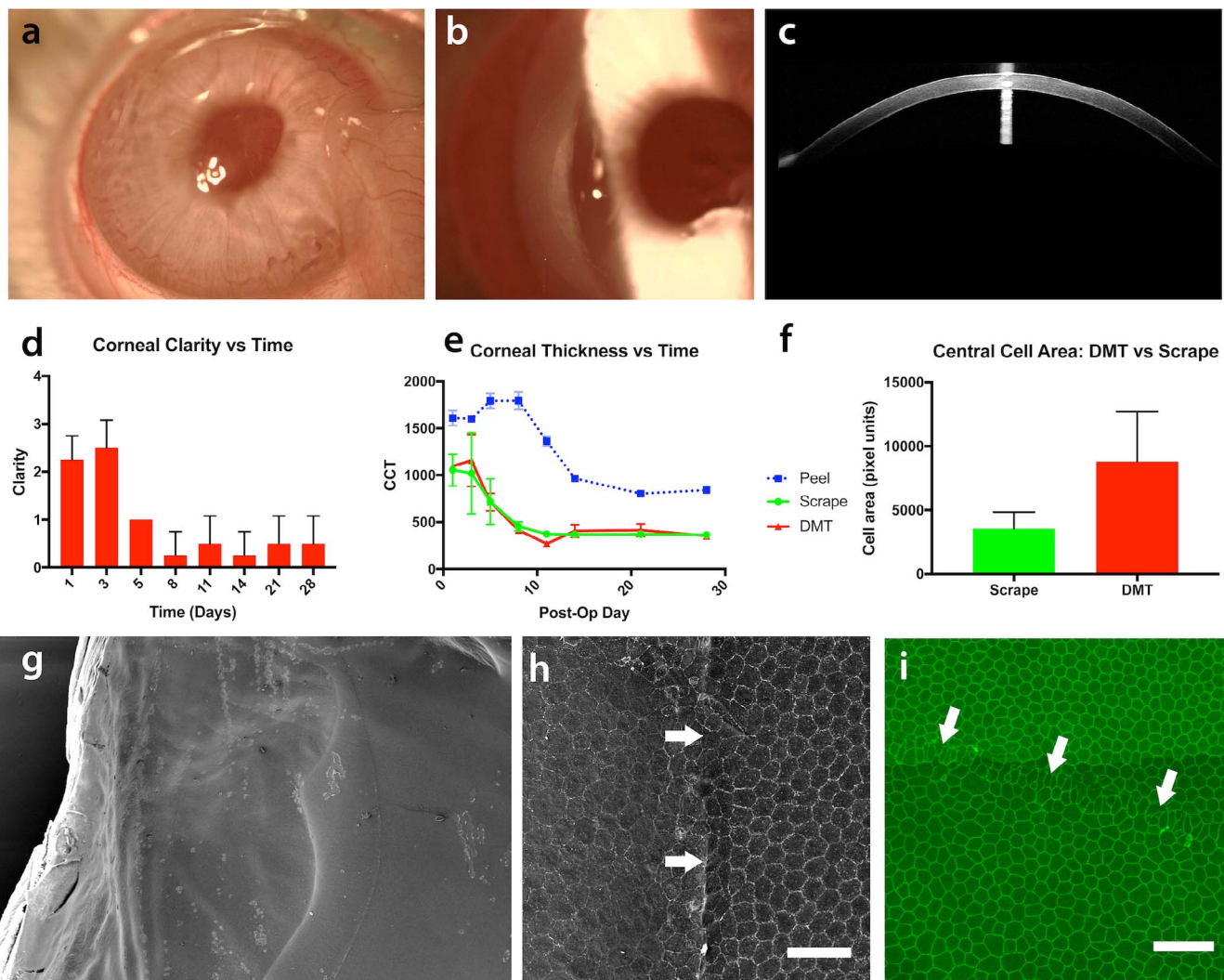


**FIGURE 7.** (a) By day 11, corneas were clear centrally in eyes after receiving Descemet's membrane transplantation. (b) An area of opacity could be seen in periphery of the graft and was most prominent just inside the descemetorhexis edge. (c) Corneal thickness and stromal reflectance did not differ significantly from control eyes on OCT examination. (d) All eyes had a central corneal clarity of 0 or 1. (e) Corneal thickness recovery matched that of the scrape wounds and was significantly better than in peel-only animals. (f) Central endothelial cell area was higher in DMT than in scrape group ( $P < 0.01$ ). (g) Endothelial cells could be seen to migrate over the Descemet's graft, forming a complete, healthy monolayer. (h) Cells could be seen to bridge Descemet's graft edge (*white arrows* represent the DM edge) on scanning electron microscopy. *Scale bar:* 50  $\mu\text{m}$ . (i) These bridging cells formed a continuous monolayer with healthy junctions as seen with ZO-1 staining on immunofluorescence. *Scale bar:* 75  $\mu\text{m}$ .

migration,<sup>27</sup> it has been postulated that the presence of guttae reduces effective endothelial cell density and consequently impedes barrier and pump function.<sup>19</sup> It has also been suggested that differences in the mechanical and chemical properties of DM in patients with FED contribute to disease progression,<sup>37</sup> and the DM in FED is known to have a different composition<sup>38</sup> and to be significantly thicker than in normal corneas.<sup>2</sup> Hence, in order to provide adequate visual rehabilitation in patients with FED, we believe that it would be necessary to remove the guttae if wound healing and vision are to be optimized. Currently, the only way to remove guttae is to strip the DM. We postulated that replacing the damaged DM with a healthy basement membrane would aid endothelial wound healing and hence we developed a new procedure that we termed "Descemet's membrane transplantation." The DMT procedure is almost identical to DMEK, meaning that surgeons familiar with this technique should easily be able to adopt it. Evidence from the literature,<sup>39,40</sup> and our own preliminary experimentation (manuscript in preparation) suggests that the

thickness of the DM does not pose a significant obstacle to endothelial migration. We chose to slightly oversize the graft, as this ensured that there was no point at which cells had to migrate over bare stroma, a process we had already determined to be associated with delayed wound healing and increased inflammation.

We found DMT restored the cell phenotype and clinical recovery back to that of the scrape group, although we did not track *in vivo* wound healing owing to concerns we could dislodge the transplant. No significant difference in corneal thickness or clarity was observed at any time point between DMT and scrape groups. However, endothelial cell size was significantly larger in the DMT group at day 28 than in the scrape group in flat mounted, *ex vivo* samples. This could be because the DMT graft was larger than the scrape wound (8.0 mm versus 7.0 mm) or it could possibly relate to differences in cell migration over human and rabbit DM, which have different mechanical properties.<sup>41</sup>

In our DMT cases, a limited, peripheral rim of scarring that originated from endothelial cells trapped between the donor and host was seen to a varying degree in all cases. This scarring was much less prominent than in the peel group and did not affect central corneal clarity. It remains to be seen if such a phenomenon occurs in humans, as this feature is not observed in DMEK when the graft overlaps the host descemetorhexis, possibly because of a difference in potential to undergo endothelial to mesenchymal transformation (EMT) in human and rabbit cells. Posterior stromal scarring has been reported in some cases of primary descemetorhexis.<sup>33,42</sup> It is possible that this relates to increased inflammation and slow recovery time, typically 2 to 6 months,<sup>43</sup> in successful primary descemetorhexis. To reduce the risk of peripheral scarring in DMT, we would advocate performing endothelial scraping in the area in which the host and donor DM overlap, removing the host endothelial cells that would be otherwise trapped in this region.

The finding that endothelial cells migrated preferentially over DM is not surprising given the importance of extracellular matrix components on successful culture of human corneal endothelial cells.<sup>44,45</sup> In addition to chemical composition, the stiffness of the substrate on which endothelial cells grow has been shown to affect cell proliferation and phenotype in vitro, with substrates mimicking the elastic modulus of DM being preferred to stiffer or softer environments.<sup>46</sup> Additionally, the surface topography of DM plays a role in enhancing endothelial proliferation and maintaining a normal phenotype.<sup>47</sup>

The importance of mechanotransduction fits with the recent elucidation that the Rho A/ROCK pathway, a signal cascade involved in sensing cell tension, is implicated in endothelial migration,<sup>22,28</sup> adhesion,<sup>48</sup> and proliferation.<sup>12,15</sup> Cell growth in vitro is also impeded when human endothelial cells are seeded onto DM from patients with PBK,<sup>49</sup> suggesting that an interplay between the structural properties of DM and endothelial cell health may be important in endothelialopathies.

Whilst DMT improved cell migration and wound healing in the rabbit model, it remains to be seen if such a strategy will prove successful in human patients with diseases of the endothelium. From our in vivo and ex vivo studies, we would expect this procedure to have an improved recovery time and success rate over other regenerative strategies, such as isolated descemetorhexis, whilst preserving the benefits of the procedure: no risk of rejection. We have recently received institutional review board approval for a clinical trial of DMT in patients with Fuchs' endothelial dystrophy and begun recruiting patients for such a study.

Whilst the procedure requires corneal tissue from which to harvest DM, the tissue does not need to have a viable endothelium, increasing the available donor pool. If successful, it may be possible to exchange donor tissue for a tissue-engineered DM substitute with modified mechanical and topographic profiles<sup>47</sup> similar to those of human DM. This could be further improved with modified surface chemistry or eluting drugs<sup>50</sup> designed to promote cell migration and proliferation.

In conclusion, we showed that corneal endothelial migration and proliferation was promoted by maintenance of a healthy basement membrane. Wound healing with a normal endothelial monolayer was a prerequisite for restoration of corneal clarity and thickness. Anatomic wound closure preceded complete physiological recovery of corneal clarity and thickness. We also described a novel surgical intervention designed to enhance endothelial cell migration in vivo, that is, DMT, which improved endothelial migration in an animal model of primary descemetorhexis.

## Acknowledgments

Supported by Medical Research Council UK research grant (MR/L002183/1) (MB).

Disclosure: **M. Bhogal**, None; **C.N. Lwin**, None; **X.-Y. Seah**, None; **G. Peh**, None; **J.S. Mehta**, None

## References

1. Meek KM, Knupp C. Corneal structure and transparency. *Prog Retin Eye Res.* 2015;49:1-16.
2. Waring GO, Bourne WM, Edelhauser HF, Kenyon KR. The corneal endothelium: normal and pathologic structure and function. *Ophthalmology.* 1982;89:531-590.
3. Joyce NC, Harris DL, Mello DM. Mechanisms of mitotic inhibition in corneal endothelium: contact inhibition and TGF-beta2. *Invest Ophthalmol Vis Sci.* 2002;43:2152-2159.
4. Joyce NC. Proliferative capacity of corneal endothelial cells. *Exp Eye Res.* 2012;95:16-23.
5. Tuft SJ, Coster DJ. The corneal endothelium. *Eye (Lond).* 1990;4(pt 3):389-424.
6. Eye Bank Association of America. 2015 Eye Banking Statistical Report. Available at: <http://restoresight.org/wp-content/uploads/2016/03/2015-Statistical-Report.pdf>.
7. Monnereau C, Quilendrino R, Dapena I, et al. Multicenter study of Descemet membrane endothelial keratoplasty: first case series of 18 surgeons. *JAMA Ophthalmol.* 2014;132:1192-1198.
8. Bourne WM. Cellular changes in transplanted human corneas. *Cornea.* 2001;20:560-569.
9. Coster DJ, Lowe MT, Keane MC, Williams KA, Australian Corneal Graft Registry Contributors. A comparison of lamellar and penetrating keratoplasty outcomes: a registry study. *Ophthalmology.* 2014;121:979-987.
10. Armitage WJ, Easty DL. Factors influencing the suitability of organ-cultured corneas for transplantation. *Invest Ophthalmol Vis Sci.* 1997;38:16-24.
11. Nakano Y, Oyamada M, Dai P, Nakagami T, Kinoshita S, Takamatsu T. Connexin43 knockdown accelerates wound healing but inhibits mesenchymal transition after corneal endothelial injury in vivo. *Invest Ophthalmol Vis Sci.* 2008;49:93-104.
12. Okumura N, Nakano S, Kay EP, et al. Involvement of cyclin D and p27 in cell proliferation mediated by ROCK inhibitors Y-27632 and Y-39983 during corneal endothelium wound healing. *Invest Ophthalmol Vis Sci.* 2014;55:318-329.
13. Koizumi N, Okumura N, Kinoshita S. Development of new therapeutic modalities for corneal endothelial disease focused on the proliferation of corneal endothelial cells using animal models. *Exp Eye Res.* 2012;95:60-67.
14. Okumura N, Koizumi N, Ueno M, et al. Enhancement of corneal endothelium wound healing by Rho-associated kinase (ROCK) inhibitor eye drops. *Br J Ophthalmol.* 2011;95:1006-1009.
15. Meekins LC, Rosado-Adames N, Maddala R, Zhao JJ, Rao PV, Afshari NA. Corneal endothelial cell migration and proliferation enhanced by Rho kinase (ROCK) inhibitors in in vitro and in vivo models. *Invest Ophthalmol Vis Sci.* 2016;57:6731-6738.
16. Fujimoto H, Maeda N, Soma T, et al. Quantitative regional differences in corneal endothelial abnormalities in the central and peripheral zones in Fuchs' endothelial corneal dystrophy. *Invest Ophthalmol Vis Sci.* 2014;55:5090-5098.
17. Brooks AM, Grant G, Gillies WE. A comparison of corneal endothelial morphology in cornea guttata, Fuchs' dystrophy and bullous keratopathy. *Aust N Z J Ophthalmol.* 1988;16:93-100.

18. Jackson AJ, Robinson FO, Frazer DG, Archer DB. Corneal guttata: a comparative clinical and specular micrographic study. *Eye (Lond)*. 1999;13(pt 6):737-743.
19. McLaren JW, Bachman LA, Kane KM, Patel SV. Objective assessment of the corneal endothelium in Fuchs' endothelial dystrophy. *Invest Ophthalmol Vis Sci*. 2014;55:1184-1190.
20. Rodrigues MM, Krachmer JH, Hackett J, Gaskins R, Halkias A. Fuchs' corneal dystrophy: a clinicopathologic study of the variation in corneal edema. *Ophthalmology*. 1986;93:789-796.
21. Giasson CJ, Solomon LD, Polse KA. Morphometry of corneal endothelium in patients with corneal guttata. *Ophthalmology*. 2007;114:1469-1475.
22. Okumura N, Koizumi N, Kay EP, et al. The ROCK inhibitor eye drop accelerates corneal endothelium wound healing. *Invest Ophthalmol Vis Sci*. 2013;54:2493-2502.
23. Jullienne R, Manoli P, Tiffet T, et al. Corneal endothelium self-healing mathematical model after inadvertent descemetorhexis. *J Cataract Refract Surg*. 2015;41:2313-2318.
24. Borkar DS, Veldman P, Colby KA. Treatment of Fuchs endothelial dystrophy by Descemet stripping without endothelial keratoplasty. *Cornea*. 2016;35:1267-1273.
25. Koenig SB. Planned descemetorhexis without endothelial keratoplasty in eyes with Fuchs corneal endothelial dystrophy. *Cornea*. 2015;34:1149-1151.
26. Watanabe S, Oie Y, Fujimoto H, et al. Relationship between corneal guttae and quality of vision in patients with mild Fuchs' endothelial corneal dystrophy. *Ophthalmology*. 2015;122:2103-2109.
27. Rizwan M, Peh GS, Adnan K, et al. In vitro topographical model of Fuchs dystrophy for evaluation of corneal endothelial cell monolayer formation. *Adv Healthc Mater*. 2016;5:2896-2910.
28. Soh YQ, Peh G, George BL, et al. Predictive factors for corneal endothelial cell migration. *Invest Ophthalmol Vis Sci*. 2016;57:338-348.
29. Mimura T, Joyce NC. Replication competence and senescence in central and peripheral human corneal endothelium. *Invest Ophthalmol Vis Sci*. 2006;47:1387-1396.
30. Bhogal M, Balda MS, Matter K, Allan BD. Global cell-by-cell evaluation of endothelial viability after two methods of graft preparation in Descemet membrane endothelial keratoplasty. *Br J Ophthalmol*. 2016;100:572-578.
31. Bhogal M, Maurino V, Allan BD. Use of a single peripheral triangular mark to ensure correct graft orientation in Descemet membrane endothelial keratoplasty. *J Cataract Refract Surg*. 2015;41:2022-2024.
32. Proulx S, Bensaoula T, Nada O, et al. Transplantation of a tissue-engineered corneal endothelium reconstructed on a devitalized carrier in the feline model. *Invest Ophthalmol Vis Sci*. 2009;50:2686-2694.
33. Arbelaez JG, Price MO, Price FW. Long-term follow-up and complications of stripping descemet membrane without placement of graft in eyes with Fuchs endothelial dystrophy. *Cornea*. 2014;33:1295-1299.
34. Treffers WF. Human corneal endothelial wound repair: in vitro and in vivo. *Ophthalmology*. 1982;89:605-613.
35. Van Horn DL, Sendele DD, Seideman S, Buco PJ. Regenerative capacity of the corneal endothelium in rabbit and cat. *Invest Ophthalmol Vis Sci*. 1977;16:597-613.
36. Okumura N, Inoue R, Okazaki Y, et al. Effect of the Rho kinase inhibitor Y27632 on corneal endothelial wound healing. *Invest Ophthalmol Vis Sci*. 2015;56:6067-6074.
37. Ali M, Raghunathan V, Li JY, Murphy CJ, Thomasy SM. Biomechanical relationships between the corneal endothelium and Descemet's membrane. *Exp Eye Res*. 2016;152:57-70.
38. Weller JM, Zenkel M, Schlötzer-Schrehardt U, Bachmann BO, Tourtas T, Kruse FE. Extracellular matrix alterations in late-onset Fuchs' corneal dystrophy. *Invest Ophthalmol Vis Sci*. 2014;55:3700-3708.
39. Hos D, Heindl LM, Bucher F, Cursiefen C. Evidence of donor corneal endothelial cell migration from immune reactions occurring after descemet membrane endothelial keratoplasty. *Cornea*. 2014;33:331-334.
40. Jacobi C, Zhivov A, Korbmayer J, et al. Evidence of endothelial cell migration after descemet membrane endothelial keratoplasty. *Am J Ophthalmol*. 2011;152:537-542.e2.
41. Danielsen CC. Tensile mechanical and creep properties of Descemet's membrane and lens capsule. *Exp Eye Res*. 2004;79:343-350.
42. Iovieno A, Neri A, Soldani AM, Adani C, Fontana L. Descemetorhexis without graft placement for the treatment of Fuchs endothelial dystrophy: preliminary results and review of the literature. *Cornea*. 2017;36:637-641.
43. Moloney G, Petsoglou C, Ball M, et al. Descemetorhexis without grafting for Fuchs endothelial dystrophy-supplementation with topical ripasudil. *Cornea*. 2017;36:642-648.
44. Choi JS, Kim EY, Kim MJ, et al. In vitro evaluation of the interactions between human corneal endothelial cells and extracellular matrix proteins. *Biomed Mater*. 2013;8:014108.
45. Okumura N, Kakutani K, Numata R, et al. Laminin-511 and -521 enable efficient in vitro expansion of human corneal endothelial cells. *Invest Ophthalmol Vis Sci*. 2015;56:2933-2942.
46. Palchesko RN, Lathrop KL, Funderburgh JL, Feinberg AW. In vitro expansion of corneal endothelial cells on biomimetic substrates. *Sci Rep*. 2015;5:7955.
47. Muhammad R, Peh GSL, Adnan K, Law JBK, Mehta JS, Yim EKF. Micro- and nano-topography to enhance proliferation and sustain functional markers of donor-derived primary human corneal endothelial cells. *Acta Biomater*. 2015;19:138-148.
48. Pipparelli A, Arsenijevic Y, Thuret G, Gain P, Nicolas M, Majo F. ROCK inhibitor enhances adhesion and wound healing of human corneal endothelial cells. *PLoS One*. 2013;8:e62095.
49. Raphael B, Lange T, Wood TO, McLaughlin BJ. Growth of human corneal endothelium on altered Descemet's membrane. *Cornea*. 1992;11:242-249.
50. Chan WY, Akhbanbetova A, Quantock AJ, Heard CM. Topical delivery of a Rho-kinase inhibitor to the cornea via mucoadhesive film. *Eur J Pharm Sci*. 2016;91:256-264.